

Absolute Rate Expressions for Hydrogen Atom Abstraction from Molybdenum Hydrides by Carbon-Centered Radicals

James A. Franz,^{*,†} John C. Linehan,^{*,†} Jerome C. Birnbaum,[†] Kenneth W. Hicks,[‡] and M. S. Alnajjar[†]

Contribution from the Pacific Northwest National Laboratory, P.O. Box 999, Richland, Washington 99352, and Norfolk State University, 2401 Corprew Avenue, Norfolk, Virginia 23504

Received April 29, 1999

Abstract: A new family of basis rate expressions for hydrogen atom abstraction by primary, secondary, and tertiary alkyl radicals in dodecane and benzyl radical in benzene from the molybdenum hydride Cp*Mo(CO)₃H and for reactions of a primary alkyl radical with CpMo(CO)₃H in dodecane are reported (Cp* = η⁵-pentamethylcyclopentadienyl, Cp = η⁵-cyclopentadienyl). Rate expressions for reaction of primary, secondary, and tertiary radical clocks with Cp*Mo(CO)₃H were as follows: for hex-5-enyl, $\log(k/M^{-1} s^{-1}) = (9.27 \pm 0.13) - (1.36 \pm 0.22)/\theta$, $\theta = 2.303RT$ kcal/mol; for hept-6-en-2-yl, $\log(k/M^{-1} s^{-1}) = (9.12 \pm 0.42) - (1.91 \pm 0.74)/\theta$; and for 2-methylhept-6-en-2-yl, $\log(k/M^{-1} s^{-1}) = (9.36 \pm 0.18) - (3.19 \pm 0.30)/\theta$ (errors are 2σ). Hydrogen atom abstraction from CpMo(CO)₃H by hex-5-enyl is described by $\log(k/M^{-1} s^{-1}) = (9.53 \pm 0.34) - (1.24 \pm 0.62)/\theta$. Relative rate constants for 1°:2°:3° alkyl radicals were found to be 26:7:1 at 298 K. Benzyl radical was found to react 1.4 times faster than tertiary alkyl radical. The much higher selectivities for Cp*Mo(CO)₃H than those observed for main group hydrides (Bu₃SnH, PhSeH, PhSH) with alkyl radicals, together with the very fast benzyl hydrogen-transfer rate, suggest the relative unimportance of simple enthalpic effects and the dominance of steric effects for the early transition-state hydrogen transfers. Hydrogen abstraction from Cp*Mo(CO)₃H by benzyl radicals is described by $\log(k/M^{-1} s^{-1}) = (8.89 \pm 0.22) - (2.31 \pm 0.33)/\theta$.

Introduction

Transition metal hydrides are particularly important chemical species because of their role in catalytic and stoichiometric hydrogenation reactions.^{1–4} Metal–hydrogen bond strengths,^{5,6} hydrogen atom^{7–11} and hydride-transfer reactions,^{12–14} and radical-mediated reduction of olefins via transition metal hydrides have been the subject of many studies.^{15–19} Although

individual rate constants for reaction of alkyl radicals with several transition metal hydrides have been reported,^{7,8,11} Arrhenius expressions have been reported only for abstraction reactions of the trityl radical with organometallic hydrides.^{9,10}

Whereas main group tin and silicon hydrides have been widely used in kinetic measurements and organic synthesis,^{20–22} transition metal hydrides have received relatively little attention as reagents for kinetic measurements and in free-radical-based synthetic transformations. Rate expressions for hydrogen abstraction from the metal hydride by organic free radicals and for the corresponding reactions of the resulting metal-centered radicals with halides and other groups provide basis rates for design and control of carbon–carbon and carbon–heteroatom bond formation in radical-based synthetic reactions.^{23,24} Thus, we present rate expressions for reactions of primary, secondary, and tertiary radical clocks and benzyl radical with molybdenum hydrides. We show that, unlike the less exothermic, but completely unselective, reactions of thiophenol and phenylselenol with primary, secondary, and tertiary alkyl radicals,^{25,26}

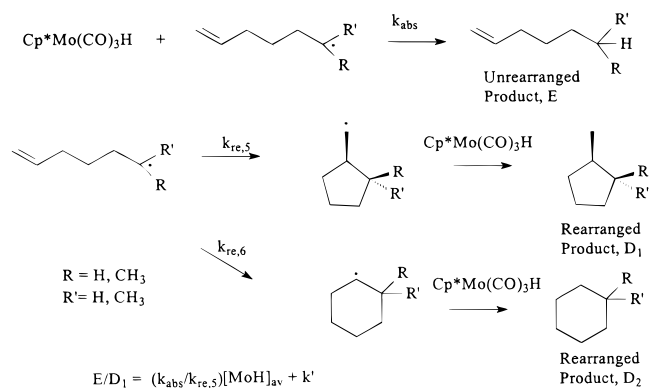
[†] Pacific Northwest National Laboratory.

[‡] Norfolk State University.

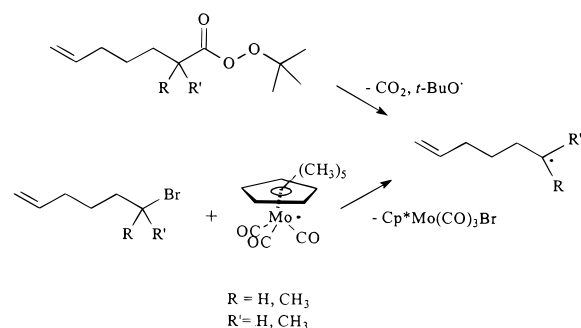
- (1) Dedieu, A. *Transition Metal Hydrides*; VCH: New York, 1992.
- (2) Moore, D. S.; Robinson, S. D. *Chem. Soc. Rev.* **1983**, *12*, 415.
- (3) Hlatky, G. G.; Crabtree, R. H. *Coord. Chem. Rev.* **1985**, *65*, 1.
- (4) Pearson, R. G. *Chem. Rev.* **1985**, *85*, 41.
- (5) Nolan, S. P.; Vega, R. L. d. I.; Hoff, C. D. *Organometallics* **1986**, *5*, 2529–2537.
- (6) Tilset, M.; Parker, V. D. *J. Am. Chem. Soc.* **1989**, *111*, 6711–6717.
- (7) Bakac, A. *Inorg. Chem.* **1998**, *37*, 3548–3552.
- (8) Ash, E. A.; Hurd, P. W.; Darensbourg, M. Y.; Newcomb, M. J. *J. Am. Chem. Soc.* **1987**, *109*, 3313–3317.
- (9) Eisenberg, D. C.; Lawrie, C. J. C.; Moody, A. E.; Norton, J. R. *J. Am. Chem. Soc.* **1991**, *113*, 4888–4895.
- (10) Eisenberg, D. C.; Norton, J. R. *Isr. J. Chem.* **1991**, *31*, 55–66.
- (11) Kinney, R. J.; Jones, W. D.; Bergman, R. G. *J. Am. Chem. Soc.* **1978**, *100*, 7902–7915.
- (12) Cheng, T.-Y.; Brunschwig, B. S.; Bullock, R. M. *J. Am. Chem. Soc.* **1998**.
- (13) Darensbourg, M. Y.; Ash, C. E. *Adv. Organomet. Chem.* **1987**, *27*, 1–50.
- (14) Kao, S. C.; Spillett, C. T.; Ash, C. L. R.; Park, Y. K.; Darensbourg, M. Y. *Organometallics* **1985**, *4*, 83–91.
- (15) Bullock, R. M.; Samsel, E. G. *J. Am. Chem. Soc.* **1990**, *112*, 6886–6898. See also the related preliminary communication: Masnovi, J.; Samsel, E. G.; Bullock, R. M. *J. Chem. Soc., Chem. Commun.* **1989**, 1044. The reversibility of the rearrangement of cyclopropylbenzyl and related radicals studied by Bullock et al. has been pointed out (Bowry, V. W.; Luszyk, J.; Ingold, K. U. *J. Chem. Soc., Chem. Commun.* **1990**, 923). This reversibility complicates quantitative interpretation of rearrangement/competition kinetic measurements in the reference cited above.

- (16) Sweany, R. L.; Halpern, J. *J. Am. Chem. Soc.* **1977**, *99*, 8335–8337.
- (17) Connolly, J. W. *Organometallics* **1984**, *3*, 1333–1337.
- (18) Garst, J. F.; Bockman, T. M.; Batlaw, R. *J. Am. Chem. Soc.* **1986**, *108*, 1689–1691.
- (19) Ungvary, F.; Marko, L. *Organometallics* **1982**, *1*, 1120–1125.
- (20) Curran, D. P. *Synthesis* **1988**, *6*, 417–439.
- (21) Baguley, P. A.; Walton, J. C. *Angew. Chem., Int. Ed. Engl.* **1998**, *37*, 7, 3072–3082.
- (22) Davies, A. G. *Organotin Chemistry*; Wiley-VCH: Weinheim, 1997.
- (23) Curran, D. P. *Adv. Free Radical Chem.* **1990**, *1*, 121–157.
- (24) Curran, D. P. *Synthesis* **1988**, *7*, 489–513.
- (25) Franz, J. A.; Bushaw, B. A.; Alnajjar, M. S. *J. Am. Chem. Soc.* **1989**, *111*, 268–275.
- (26) Newcomb, M.; Choi, S.-Y.; Horner, J. H. *J. Org. Chem.* **1999**, *64*, 1225.

Scheme 1



Scheme 2



$Cp^*Mo(CO)_3H$ exhibits appreciable selectivity in abstraction reactions, reflecting a trend, primary > secondary > benzyl > tertiary, that is predominately steric, rather than enthalpic, in origin. The present kinetic results offer a new family of basis rate expressions for hydrogen-transfer reactions of alkyl and benzyl radicals for use in competition kinetics and the design of radical-based synthetic strategies.

Results

Alkyl Radical Clock Kinetics. The rates of hydrogen atom abstraction from $Cp^*Mo(CO)_3H$ and $CpMo(CO)_3H$ by alkyl radicals were determined using the appropriate alkenyl radical clocks (Scheme 1).²⁷ For primary and tertiary clock radicals, an integrated rate expression which accounts for changing hydride concentration was employed to determine the relative rate constants for radical clock rearrangement vs abstraction, k_{rel} , where $k_{rel} = k_{re}/k_{abs}$. The abstraction rate constants, k_{abs} , were determined from ratios of concentrations of unrearranged, reduced hydrocarbon to rearranged hydrocarbon using values of k_{re} from Arrhenius rate expressions for the clock reactions available in the literature.^{28,29} Both alkenyl bromides and *tert*-butyl peresters of alkenoic acids were used to generate the desired primary and tertiary radicals in reactions with $Cp^*Mo(CO)_3H$ (Scheme 2). The ring-unsubstituted hydride $CpMo(CO)_3H$ was found to react rapidly at room temperature with peresters to produce exclusively alkenoic acids and *tert*-butyl alcohol, and thus bromide radical precursors rather than perester radical precursors were employed with this hydride.

The rates of abstraction by a secondary radical clock from $Cp^*Mo(CO)_3H$ were determined using the alkenyl bromide secondary clock precursor by a linear fit of the ratio of

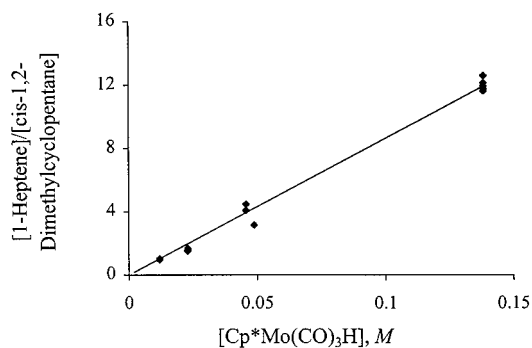


Figure 1. Plot of un-rearranged (1-heptene) to rearranged reduced hydrocarbon (*cis*-1,2-dimethylcyclopentane) as a function of hydride donor concentration at 373 K.

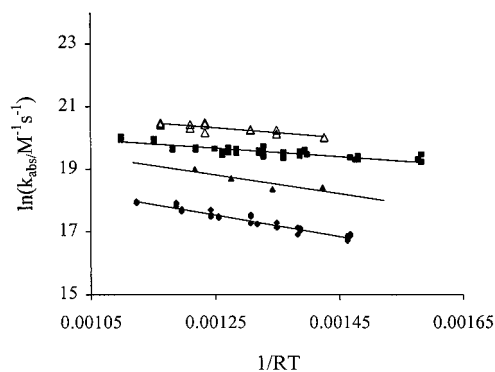


Figure 2. Arrhenius plots for the abstraction of a hydrogen atom from molybdenum hydrides by primary, secondary, and tertiary alkyl radicals in dodecane. The abstraction from $Cp^*Mo(CO)_3H$ by hex-5-enyl (■), by hept-6-en-2-yl (▲), and by 2-methylhept-6-en-2-yl (◆) and the abstraction from $CpMo(CO)_3H$ by hex-5-enyl (△) are shown.

unrearranged product (1-heptene, *E* in Scheme 1) to the major rearranged product (*cis*-1,2-dimethylcyclopentane, *D*₁ in Scheme 1) vs molybdenum hydride concentrations at short (<10%) extent of conversion of hydride. The values of k_{abs} at each temperature were calculated from the slope of the plot of E/D_1 vs $Cp^*Mo(CO)_3H$ concentrations, slope = k_{abs}/k_{re} , with values of k_{re} available from the literature Arrhenius values.^{28,29} An example of a plot of the ratio of unrearranged to rearranged product (E/D_1 , Scheme 1) as a function of molybdenum hydride concentration at short extent of hydride conversion for the reaction of hept-6-en-2-yl with $Cp^*Mo(CO)_3H$ at 373 K is shown in Figure 1. This treatment corrects for the presence of secondary hydrogen-donating processes, represented by k' , where $k' = k_{abs}'[DH']$. Here, DH' is an adventitious hydrogen donor and k_{abs}' is the associated rate constant for abstraction. A near-zero intercept k' indicates the lack of significant hydrogen sources in the solvent, or other alternate sources of the unrearranged hydrocarbon not proportional to the primary donor concentration.

The Arrhenius plots of data for the reaction of $Cp^*Mo(CO)_3H$ with primary, secondary, and tertiary radicals are presented in Figure 2. These plots include results from both alkenyl bromide and perester radical precursors for the primary and tertiary radicals, while the secondary radical rate was determined using the bromide clock precursor. The Arrhenius and Eyring parameters for hydrogen abstraction from $Cp^*Mo(CO)_3H$ by alkyl radicals are presented in Table 1.

Both perester and bromide precursors were used over the entire temperature range and gave identical results within statistical error limits. Unlike the rapid iodine atom-exchange reactions between radicals and organic iodides, which may

(27) Griller, D.; Ingold, K., U. *Acc. Chem. Res.* **1980**, *13*, 317–323.

(28) Chatgililoglu, C.; Ingold, K. U.; Scaiano, J. C. *J. Am. Chem. Soc.* **1981**, *103*, 7739–7742.

(29) Luszytk, J.; Maillard, B.; Deycard, S.; Lindsay, D. A.; Ingold, K. U. *J. Org. Chem.* **1987**, *52*, 3509–3514.

Table 1. Arrhenius^a and Eyring Parameters for the Reaction of Primary, Secondary, and Tertiary Radical Clocks^b and Benzyl Radicals with Cp*Mo(CO)₃H and Primary Radicals with CpMo(CO)₃H in Dodecane^c

radical	hydride	log A (M ⁻¹ s ⁻¹)	ΔS [‡] (eu) (T _m , K)	E _a (kcal/mol)	ΔH [‡] (kcal/mol)	k (M ⁻¹ s ⁻¹), 298 K	temp range (K)	mean temp (T _m , K)
hex-5-enyl	Cp*Mo(CO) ₃ H	9.27 ± 0.13	-19.8 ± 1.7	1.36 ± 0.22	0.61 ± 0.20	1.9 × 10 ⁸	319–400	384
hept-6-en-2-yl	Cp*Mo(CO) ₃ H	9.12 ± 0.42	-19.3 ± 2.3	1.91 ± 0.74	1.15 ± 0.71	5.2 × 10 ⁷	318–458	387
2-methylhept-6-en-2-yl	Cp*Mo(CO) ₃ H	9.36 ± 0.18	-18.2 ± 1.7	3.19 ± 0.30	2.42 ± 0.30	1.1 × 10 ⁷	343–448	390
hex-5-enyl	CpMo(CO) ₃ H	9.53 ± 0.34	-17.5 ± 1.2	1.24 ± 0.62	0.47 ± 0.63	4.2 × 10 ⁸	318–458	399
benzyl	Cp*Mo(CO) ₃ H	8.89 ± 0.22	-20.0 ± 2.0	2.31 ± 0.33	1.65 ± 0.39	1.5 × 10 ⁷	297–373	325

^a Eyring and Arrhenius parameters are related by $\Delta H^\ddagger = -R(\partial \ln(k_{\text{abs}}/T)/\partial(1/T)) = E_a - RT_m$, where T_m is the mean temperature of the kinetics, and $\Delta S^\ddagger = R(\ln(hk_{\text{abs}}/k_b T_m)) + \Delta H^\ddagger/T_m = R \ln(hA/e k_b T_m)$, where k_b is Boltzmann's constant, h is Planck's constant, k_{abs} is the rate constant from the Arrhenius expression at mean temperature, and e is the base of natural logarithms. ^b The radical cyclization rates used in this work are (ref 29): for hex-5-enyl, $\log(k_{\text{c},s}/s^{-1}) = 10.42 - 6.85/\theta$, $\theta = 2.303RT$ kcal/mol; for hept-6-en-2-yl, cyclization to *cis*-2-methylcyclopentylmethyl is given by $\log(k_{\text{c},cis}/s^{-1}) = 9.79 - 6.50/\theta$ and to *trans*-2-methylcyclopentylmethyl is given by $\log(k_{\text{c},trans}/s^{-1}) = 9.92 - 7.44/\theta$; for 2-methyl-hept-en-2-yl, $\log(k_{\text{c},s}/s^{-1}) = 10.0 - 6.1/\theta$. ^c The reaction of benzyl radical with Cp*Mo(CO)₃H was carried out in benzene. Errors are 2σ.

compromise unrearranged/rearranged hydrocarbon ratios³⁰ and affect their use in synthetic transformations,³¹ bromine atom exchange between the alkenyl bromides and the cyclized radical is unimportant, reflected in the present results, that show close agreement between perester and bromide precursors.

The Arrhenius plot for hydrogen abstraction from CpMo(CO)₃H by hex-5-enyl is also shown in Figure 2, and the rate expression for abstraction of hydrogen by the primary clock from CpMo(CO)₃H is presented in Table 1.

Benzyl Radical Kinetics. Rate constants for hydrogen abstraction by the benzyl radical from Cp*Mo(CO)₃H were determined by a competition of abstraction to form toluene with benzyl radical self-termination to produce bibenzyl during photolysis of dibenzyl ketone (DBK) in benzene solutions. The benzyl radical was produced by broadband visible UV irradiation (>330 nm) of optically dilute solutions of the ketone and hydride, as shown in Scheme 3. Figure 3 shows the time-dependent evolution of products during photolysis of a 0.02 M solution of DBK in benzene at 373 K.

Under conditions of constant rate of photolysis of dibenzyl ketone, the absence of photolysis of starting hydride, and no significant absorption of light by photoproducts, the relationship between toluene, bibenzyl (BB), and the initial hydride concentration, [MoH]₀, that accounts for consumption of MoH is given by eq 1a. At low conversion of hydride, the exponent term, $k_{\text{abs}}[\text{BB}]^{1/2}\Delta t^{1/2}/k_t^{1/2}$ in eq 1a is small, and simplifies to eqs 1b and 1c, where [MoH]_{av} represents the average concentration of the molybdenum hydride over a period of photolysis time, Δt:

$$[\text{toluene}] = [\text{MoH}]_0(1 - e^{-k_{\text{abs}}[\text{BB}]^{1/2}\Delta t^{1/2}/k_t^{1/2}}) \quad (1a)$$

$$[\text{toluene}] = [\text{MoH}]_0 \left(\frac{k_{\text{abs}}[\text{BB}]^{1/2}\Delta t^{1/2}}{k_t^{1/2}} \right) \quad (1b)$$

$$k_{\text{abs}} = \frac{[\text{toluene}]k_t^{1/2}}{[\text{BB}]^{1/2}[\text{MoH}]_{\text{av}}\Delta t^{1/2}} \quad (1c)$$

In practice, conversion of hydride up to 35% leads to less than about 10% error in rate constant k_{abs} using eq 1c. In the present experiments, the yield of toluene was used to calculate an average hydride concentration at each photolysis time. Combining experimental values of bibenzyl and toluene at 0.5, 1.0, and 1.5 s photolysis time with an independent value of the rate constant for self-termination of bibenzyl, k_t (see below), provided values of k_{abs} at each temperature.

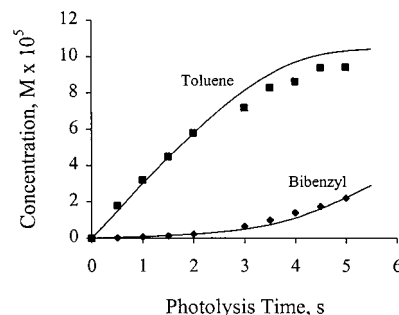
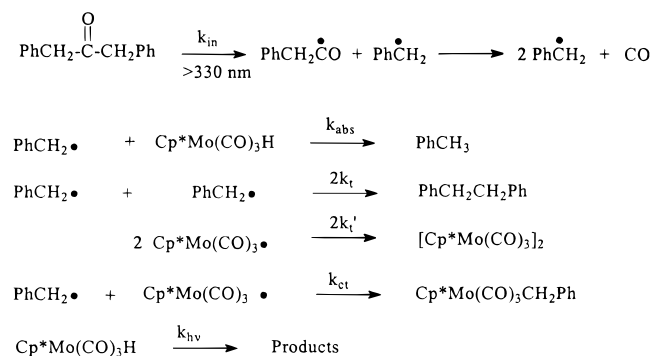


Figure 3. Product evolution of toluene (■) and bibenzyl (◆) at 373 K at initial concentrations of [Cp*Mo(CO)₃H], 0.000105 M, and [dibenzyl ketone], 0.02 M. Rate constants are determined using data at 0.5, 1.0, and 1.5 s and eq 1c. The solid lines are the predicted concentrations of toluene and bibenzyl from minimizing the sum of the squares of residuals for toluene and bibenzyl in a numerical integration of Scheme 3 using a rate constant for photolysis of DBK, 8.7×10^{-6} M/s, $k_t = 0.5k_{\text{ct}} = k_t' = 6.2 \times 10^9$ M⁻¹ s⁻¹, giving $k_{\text{abs}} = 3.44 \times 10^7$ M⁻¹ s⁻¹. The agreement of the two approaches is due to the near linearity of the product curves through about 50% conversion of hydride. All of the points of Figure 3 can be alternatively fit to eq 1a, allowing k_{abs} and the initial hydride concentration (MoH) to vary in a nonlinear least-squares optimization. This results in a predicted initial concentration of hydride of 9.13×10^{-5} M and a rate constant $k_{\text{abs}} = 3.46 \times 10^7$ M⁻¹ s⁻¹. Alternatively, the first three points (0.5, 1.0, and 1.5 s) can be fit to eq 1a. This results in values of k_{abs} identical to those resulting from an average of 0.5, 1.0, and 1.5 s points using eq 1c.

Scheme 3



The rate of photolysis of DBK employed in the kinetic measurements was in the range [DBK] × (7–9) × 10⁻⁶ s⁻¹, corresponding to a steady-state concentration of benzyl radical in the range (2–5) × 10⁻⁸ M. The rate of formation of toluene and bibenzyl was found to be approximately linear during the first 2 s of photolysis. The evolution of toluene and bibenzyl with time was examined by numerical integration of the

(30) Newcomb, M.; Curran, D. P. *Acc. Chem. Res.* **1988**, *21*, 206–214.

(31) Curran, D. P. *NATO ASI Ser., Ser. C* **1989**, *260* (*Free Radicals Synth. Biol.*), 37–51.

equations of Scheme 3. In general, it was found that toluene and bibenzyl formation was accurately predicted through about 50% conversion of hydride using the experimentally measured initial concentration of hydride in the numerical integration. At longer reaction times, toluene production is less than that predicted by typically 10% (see Figure 3). This may be due to several circumstances, including (1) the presence of less hydride initially in the photolysis, (2) partial photolysis of the hydride to a non-hydrogen-donating species during the course of the reaction, (3) a decrease in the rate of photolysis due to light absorption by the products, or (4) more complex photochemistry of the system at high conversion. The photochemistry of $\text{Cp}^*\text{Mo}(\text{CO})_3\text{H}$ involves CO loss and subsequent reactions of the 16-electron $\text{Cp}^*\text{Mo}(\text{CO})_2\text{H}$.³² Photolysis of the dimer $[\text{Cp}^*\text{Mo}(\text{CO})_3]_2$ results in CO loss, giving $\text{Cp}_2\text{Mo}_2(\text{CO})_5$ or metal–metal bond homolysis to form the radical $\text{Cp}^*\text{Mo}(\text{CO})_3$.³³ In the benzyl radical experiments, a 1-kW high-pressure (Pyrex-filtered) xenon arc lamp was used. Those conditions led to a small extent of photolysis (<10%) of the hydride during the kinetic experiments, whereas in the experiments utilizing halide radical clock precursors, the Pyrex-filtered, diffuse light of a 100-W long-wavelength sunlamp ($\lambda_{\text{max}} = 365 \text{ nm}$) was employed, which led to significant photolysis of the hydride only after prolonged photolysis. (In the halide radical clock precursor experiments, radical initiation most probably occurred via photolysis of small amounts of the dimer $[\text{Cp}^*\text{Mo}(\text{CO})_3]_2$ present in the hydride $\text{Cp}^*\text{Mo}(\text{CO})_3\text{H}$.) Kinetic modeling of case 1, by reducing the initial hydride concentration, or of case 2, by adding an additional decay pathway in the numerical integration of the equations of Scheme 3 (k_{hv} in Scheme 3), produced an overall better fit of the data through complete consumption of hydride but poorer agreement with the experimental concentrations of hydride used and poorer agreement with initial rates of reaction calculated using eq 1c. Careful analysis of material balances revealed no more than 6–7% decrease in the rate of photolysis of DBK over 5 s; thus, case 3 was found insignificant. Because of the small discrepancy at longer photolysis times, we preferred to use eq 1c for data obtained through typically 1.5 s, or less than one half-life of hydride conversion, to avoid ambiguities of modeling the system at high conversion. For times between 0.5 and 1.5 s, values of k_{abs} found by numerical integration (Scheme 3, neglecting k_{hv}) were found to be in excellent agreement with the rates calculated with eq 1c from initial product ratios ($[\text{PhCH}_3]/[\text{PhCH}_2\text{CH}_2\text{Ph}]^{1/2}$) when the kinetic simulation employs k_{abs} as the only variable and values of k_t , rate of photolysis of DBK, and hydride concentration are experimental constants. The Arrhenius plot for reaction of benzyl radical with $\text{Cp}^*\text{Mo}(\text{CO})_3\text{H}$ is shown in Figure 4, and the rate expression is presented in Table 1.

Discussion

Alkyl and Benzyl Radical Selectivities in Hydrogen Atom Abstractions of Molybdenum Hydrides. The rate constant for hydrogen atom abstraction by a primary radical from $\text{Cp}^*\text{Mo}(\text{CO})_3\text{H}$ at 298 K ($1.9 \times 10^8 \text{ M}^{-1} \text{ s}^{-1}$) is similar in magnitude to rates of abstraction of alkyl radicals from thiophenol: e.g., for the reaction of *n*-butyl radical with thiophenol, $k_{\text{abs}} = 1.4 \times 10^8 \text{ M}^{-1} \text{ s}^{-1}$ and is about an order of magnitude less than that for phenylselenol.^{25,26} Thiophenol and phenylselenol have the useful properties (as kinetic radical trapping agents) of exhibiting, within experimental error, no selectivity between

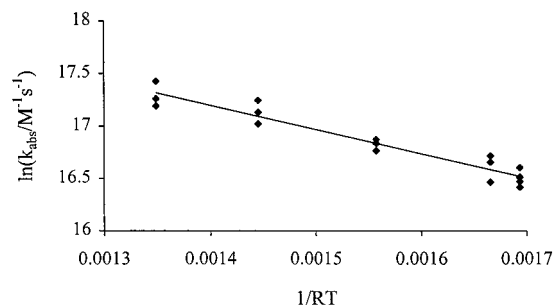


Figure 4. Arrhenius data for abstraction of hydrogen by benzyl radical from $\text{Cp}^*\text{Mo}(\text{CO})_3\text{H}$, calculated using eq 1c from toluene and bibenzyl from photolysis times of 0.5–1.5 s in benzene.

tertiary, secondary, and primary alkyl radicals. Relative rates for tertiary, secondary, and primary and benzyl radicals are shown in Table 2 for thiophenol,²⁵ phenylselenol,²⁶ and tributylstannane. The S–H and Se–H bond strengths of thiophenol and phenylselenol are $80 \pm 2 \text{ kcal/mol}$ ^{34–36} and $78 \pm 2 \text{ kcal/mol}$,³⁷ respectively. The M–H bond strengths of $\text{Cp}^*\text{Mo}(\text{CO})_3\text{H}$ and $\text{CpMo}(\text{CO})_3\text{H}$ are 69 and 70 kcal/mol, respectively.^{5,6,38} Table 2 illustrates that the relative magnitudes of rate constants and activation barriers for highly exothermic hydrogen abstraction reactions are not related by simple enthalpy considerations. For main group hydrides, stabilized radicals react more slowly than simple alkyl radicals. Thus, benzyl radical abstracts hydrogen atom about 2–300 times more slowly from PhSH and Bu_3SnH than alkyl radicals, reflecting the trend in C–H bond dissociation energies for primary (1-propyl C–H), secondary (2-propyl C–H), tertiary (*tert*-butyl C–H), and benzyl (toluene α C–H) radicals: 101, 99, 95, and 89 kcal/mol, respectively.^{39–41} Thus, the selectivity of alkyl radicals in the much more highly exothermic reactions of $\text{Cp}^*\text{Mo}(\text{CO})_3\text{H}$ with alkyl radicals is quite remarkable compared to the selectivity in reactions of primary, secondary, and tertiary alkyl radicals with PhSH, Bu_3SnH , and PhSeH. The relative reactivity of benzyl radical with $\text{Cp}^*\text{Mo}(\text{CO})_3\text{H}$ is also surprising by comparison with the main-group hydrides, exhibiting a rate constant higher than that of tertiary alkyl radical. Since the benzyl radical is slower than the secondary alkyl radical, enthalpic effects are almost, but not completely, removed. The results of Table 2 suggest that the selectivity of the hydrogen abstraction reactions of $\text{Cp}^*\text{Mo}(\text{CO})_3\text{H}$ can be attributed in significant extent to metal ligand/radical steric effects. In comparing the results of thiophenol and $\text{Cp}^*\text{Mo}(\text{CO})_3\text{H}$ in Table 2, it will be noted that the reaction of benzyl radical with $\text{Cp}^*\text{Mo}(\text{CO})_3\text{H}$ ($\Delta H^\circ \approx -20 \text{ kcal/mol}$) is similar in exothermicity to the reaction of secondary ($\Delta H^\circ \approx -21 \text{ kcal/mol}$) or tertiary radical ($\Delta H^\circ \approx -19 \text{ kcal/mol}$)^{39–41} with PhSH.

Several examples of the steric effects of pentamethyl substitution of the cyclopentadiene group in homolytic displacement and atom-transfer chemistry can be cited. In the present work,

(34) Colussi, A. J.; Benson, S. W. *Int. J. Chem. Kinet.* **1977**, *9*, 925.

(35) McMillen, D. F.; Golden, D. M. *Annu. Rev. Phys. Chem.* **1982**, *33*, 493.

(36) Bordwell, F. G.; Xian-Man, Z.; Satish, A. V.; Cheng, J.-P. *J. Am. Chem. Soc.* **1994**, *116*, 6605–6610.

(37) Leech, D. T.; Li, R.; Chyall, L. J.; Kentaemaa, H. I. *J. Phys. Chem.* **1996**, *100*, 6608–6611.

(38) Tilset, M. P.; Vernon B. *J. Am. Chem. Soc.* **1990**, *112*, 2843.

(39) Tsang, W. In *Heats of Formation of Organic Free Radicals by Kinetic Methods*; Simões, J. A. M., Greenberg, A., Liebman, J. F., Eds.; Blackie Academic & Professional: New York, 1996; Vol. 4, pp 22–58.

(40) Lias, S. G.; Bartness, J. E.; Liebman, J. F.; Holmes, J. L.; Levin, R. D.; Mallard, W. G. *J. Phys. Chem. Ref. Data* **1988**, *17*, Suppl. 1.

(41) Seakins, P. W.; Pilling, M. J.; Niiranen, J. T.; Gutman, D.; Krasnaperov, L. N. *J. Phys. Chem.* **1992**, *96*, 9847.

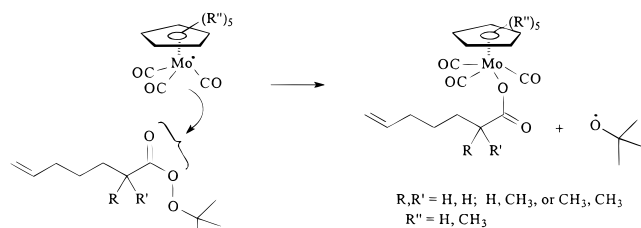
(32) Mahmoud, K. A. R.; Anthony J.; Alt, H. G. *J. Chem. Soc., Dalton Trans.* **1984**, 187–197.

(33) Peters, J. G.; Michael W.; Turner, J. J. *Organometallics* **1995**, *14*, 1503–1506.

Table 2. Absolute Rates and Selectivities for Reaction of Alkyl and Benzyl Radicals with Hydrides

hydrogen donor	X–H BDE kcal/mol	absolute rates of hydrogen abstraction at 298 K ($M^{-1} s^{-1}$)				relative rates of hydrogen abstraction at 298 K			
		1° radical	2° radical	3° radical	benzyl	1° radical	2° radical	3° radical	benzyl
$Cp^*Mo(CO)_3H^a$	70 ^e	1.9×10^8	5.2×10^7	1.1×10^7	1.5×10^7	25.5	7.0	(1)	1.4
Bu_3SnH^b	74, ^f 78 ⁱ	2.4×10^6	1.8×10^6	1.8×10^6	3.6×10^4	1.3	1.0	(1)	2.0×10^{-12}
$PhSH^c$	80 ^s	1.1×10^8	1.05×10^8	1.14×10^8	3.1×10^5	1.0	0.9	(1)	2.7×10^{-2}
$PhSeH^d$	78 ^h	1.3×10^9	1.1×10^9	1.3×10^9	–	1.0	0.85	(1)	–

^a This work. Alkyl radical rates were measured in alkane solvent, and benzyl radical rates were determined in benzene; see Experimental Section. ^b Rate determined in alkane–trialkylphosphine/di-*tert*-butylperoxide media; see ref 28. ^c Rate measurements in hydrocarbons; see ref 25. ^d Rate measurements in tetrahydrofuran: Newcomb, M.; Choi, S.-Y.; Horner, J. H. *J. Org. Chem.* **1999**, *64*, 1225. ^e References 5 and 6. ^f Burkey, T. J.; Majewski, M.; Griller, D. *J. Am. Chem. Soc.* **1986**, *108*, 2218–2221. Jackson, R. A. *J. Organomet. Chem.* **1979**, *166*, 17. ^g References 34–36. ^h Reference 37. ⁱ Laarhaven, L. J. J.; Mulder, P.; Wayner, D. D. M. *Acc. Chem. Res.* **1999**, *32*, 342–349.

Scheme 4

$CpMo(CO)_3H$ reacts an additional factor of 1.9 faster than $Cp^*Mo(CO)_3H$ with primary radicals. Pentamethyl substitution at Cp has been shown to attenuate the rate of reaction of hydrides in reactions with tris(*p*-*tert*-butylphenyl)methyl radical.⁹ Ligand-based steric effects were noted on the rates of hydrogen atom abstraction from macrocyclic rhodium hydrides by methyl radicals.⁷ Hydrogen abstraction from PhSH and PhSeH is unselective, because the single ligand of the divalent sulfides and selenides presents minimal steric interaction with the attacking radical centers. Lacking appreciable steric interaction of the selenide with substituents about the alkyl radical, alkyl radicals react with PhSeH at partially diffusion-controlled rates, independent of the exothermicity of the reaction for primary, secondary, and tertiary alkyl radicals.^{42–46} In general, more pronounced steric effects are typically observed for higher coordination number transition metal complexes in homolytic displacement reactions than for main-group organometallic radicals. Appropriate choice of ligand on tin hydrides and reduced substrate leads to appreciable stereoselectivity in tin hydride-based reductions,²¹ and the replacement of a carbonyl ligand by a bulkier ligand decreased the rate of hydrogen atom transfer significantly (by 200-fold) for $HMn(CO)_5$ (Mn–H BDE = 68 kcal/mol) vs $HMn(PEtPh_2)(CO)_4$ (Mn–H BDE = 71 kcal/mol) at 298 K.⁹

Induced Decomposition of Peresters by Molybdenum Hydrides. The peresters used in this study, *tert*-butyl 2,2-dimethylperhept-6-enoate, *tert*-butyl 2-methylperhept-6-enoate, and *tert*-butyl perhept-6-enoate, were found to undergo reaction with $Cp^*Mo(CO)_3H$ to give the corresponding molybdenum alkenoate acid complexes in competition with unimolecular thermal decomposition of the perester to give alkyl radicals (Scheme 4). The induced decomposition is most probably a chain reaction, involving attack of the molybdenum-centered

radicals on the peresters to produce the molybdenum carboxylate complexes. $CpMo(CO)_3H$ reacted completely with all three peresters at room temperature before the samples could be sealed for kinetic experiments, whereas no significant reduction of the peresters by $Cp^*Mo(CO)_3H$ occurred at room temperature. At higher temperatures, both the induced decomposition pathway and the desired unimolecular decomposition of the peresters occur with $Cp^*Mo(CO)_3H$. In the kinetic studies employing the peresters, a correction for hydride consumption through induced decomposition was made by careful analysis of the excess yield of *tert*-butyl alcohol formed over reduced radical products. The trimethylsilyl derivative of the tertiary acid, 2-methylhept-6-enoic acid, was identified after treatment of the reaction mixture with bis(trimethylsilyl)acetamide (BSA) and pyridine. The amount of the silylated acid corresponded closely to the difference between the alcohol concentration and the total hydrocarbon concentration. It is assumed that the product alkenoic acid was present in the solution as a molybdenum carboxylate complex.^{47,48}

The efficiency of the induced decomposition pathway of the peresters in reaction with $Cp^*Mo(CO)_3H$ decreased with α -alkyl substitution of the peresters. The perester precursor of hex-5-enyl radical underwent 99% reduction at 97 °C, the secondary 96% at 72 °C, and the tertiary 70% at 70 °C. At higher temperatures (> 120 °C), the rate of unimolecular decomposition of the tertiary and secondary peresters is sufficiently fast to provide ample radical production compared to the induced decomposition pathway of reduction by $Cp^*Mo(CO)_3H$. Note that the site of the reaction of molybdenum radicals, carbonyl or peroxidic oxygen, is not specified in Figure 4. Although $CpMo(CO)_3^*$ radical is known to react at the carbonyl groups of quinones,^{49,50} reactions of alkyl and other radicals with peresters have been established to occur at the peroxidic oxygen.⁵¹ Whether attack occurs at carbonyl or peroxidic oxygen, the efficiency of the induced decomposition pathway suggests that pyridinethiocarboxylic acid esters, employed as convenient radical precursors,²⁶ will also be useful as radical precursors in conjunction with the molybdenum hydrides.

Conclusions

A new family of rate expressions using transition metal hydrides has been developed for use in competition kinetics and radical-based synthetic transformations, and for estimation

(42) Newcomb, M.; Manek, M. B. *J. Am. Chem. Soc.* **1990**, *112*, 9662–9663.

(43) Newcomb, M.; Johnson, C. C.; Manek, M. B.; Varick, T. R. *J. Am. Chem. Soc.* **1992**, *114*, 10915–10921.

(44) Martin-Esker, A. A.; Johnson, C. C.; Horner, J. H.; Newcomb, M. *J. Am. Chem. Soc.* **1994**, *116*, 9174–9181.

(45) Le Tadic-Biadatti, M. H.; Newcomb, M. *J. Chem. Soc., Perkin Trans. 2* **1996**, 1467–1473.

(46) Newcomb, M.; Varick, T. R.; Ha, C.; Manek, M. B.; Yue, X. *J. Am. Chem. Soc.* **1992**, *114*, 8158–8163.

(47) Cotton, F. A.; Darenbourg, D. J.; Kolthammer, B. W. S. *J. Am. Chem. Soc.* **1981**, *103*, 398–405.

(48) Garner, C. D.; Hughes, B. *Adv. Inorg. Chem. Radiochem.* **1975**, *17*, 1.

(49) Hanaya, M.; Tero-Kubota, S.; Iwazumi, M. *Organometallics* **1988**, *7*, 1500–1504.

(50) Hanaya, M.; Kwaizumi, M. *Organometallics* **1989**, *8*, 672–676.

(51) Ingold, K. U.; Roberts, B. P. *Free-Radical Substitution Reactions; Bimolecular Homolytic Substitutions (S_H2 Reactions) at Saturated Multi-valent Atoms*; Wiley-Interscience: New York, 1971.

of fundamental steps in hydrogen transfer involving the molybdenum hydride group in the context of catalysis. The rate constants for hydrogen abstraction from Cp*Mo(CO)₃H and CpMo(CO)₃H by alkyl radicals, and the efficiency of induced decomposition reactions of the corresponding molybdenum radicals Cp*Mo(CO)₃[•] and CpMo(CO)₃[•] in reactions with peresters, have been shown to be influenced by the steric bulk of the metal ligands and the α-alkyl substituents on the radical center, or by the effects of α-alkyl substitution of the perester. The influence of steric interactions on the rates of highly exothermic reactions of the hydrides with carbon-centered radicals is generally recognized.¹⁰

Experimental Section

CpMo(CO)₃H,⁵² Cp*Mo(CO)₃H,⁵² 6-bromoheptene,⁵³ 2,2-dimethylhept-6-enoic acid,⁵⁴ 2-chloro-2-methylhept-6-ene,⁵⁵ and 2-bromo-2-methylhept-6-ene⁵⁶ were synthesized using modified literature procedures. 2-Methylhept-6-enoic acid and hept-6-enoic acid were synthesized in a manner similar to that used for 2,2-dimethylhept-6-enoic acid.⁵⁴

tert-Butyl 2,2-Dimethylperhept-6-enoate. The acid chloride was produced by refluxing 2,2-dimethylhept-6-enoic acid with excess SOCl₂ in CH₂Cl₂, to give the acid chloride, >95% purity by NMR. ¹H NMR, CDCl₃: δ 1.31 (6H, s), 1.41 (2H, m), 1.68 (2H, m), 2.10 (2H, m), 5.03 (2H, m), 5.81 (1H, m). ¹³C NMR: δ 23.85 (1C), 25.17 (2C), 33.82 (1C), 39.74 (1C), 52.79 (1C), 115.10 (1C), 137.95 (1C), 180.23 (1C). The acid chloride was converted to the perester by reaction with tert-butyl hydroperoxide in CH₂Cl₂ at 0 °C. Chromatography of the crude perester on silica gel using 2.5% methyl tert-butyl ether in pentane gave a fraction containing pure liquid perester, 0.48 g (17% yield).

tert-Butyl perhept-6-enoate and tert-butyl 2-methylhept-6-enoate were similarly prepared as clear liquids in 25–55% isolated yields.

tert-Butyl 6-perheptenoate: ¹³C NMR (CDCl₃) δ 24.20 (1C), 25.93 (3C), 28.01 (1C), 30.88 (1C), 33.05 (1C), 83.06 (1C), 114.71 (1C), 137.93 (1C), 170.81 (1C).

tert-Butyl 2-methylperhept-6-enoate: ¹³C NMR (CDCl₃) δ 173.89 (C(O)O), 138.17 (CH₂=CH–), 114.81 (CH₂=CH–), 83.22 (O–C(CH₃)), 37.21 (–C(CH₃)H–), 33.38 (–CH₂–), 33.16 (–CH₂–), 26.39 (–CH₂–), 26.12 (C(CH₃)₃), 17.40 (CH(CH₃)).

Kinetic Procedure for Alkyl Radical Clock Kinetics. Solutions of halide or perester radical precursor, hydride, and internal GC standard were freeze–thaw degassed, sealed in Pyrex tubes, and heated through four half-lives of the peresters or heated and photoinitiated (halide precursors) with a tungsten filament lamp. The usual integrated rate expression,^{57,58} eq 2, with a correction factor for consumption of hydride, *f*, was used to determine the relative rate constants for the radical clock experiments:

$$E + D = 1/f(B_0 + r)(1 - e^{-fD/r}) \quad (2)$$

$$f = 1 + \frac{[t\text{-BuOH}]}{(E + D)} \quad (3)$$

*B*₀ is the initial hydride concentration, *D* is the sum of rearrangement products, and *E* is the concentration of unrearranged reduced hydrocarbon. Equation 2 is solved by computer for the relative rate, *r* = *k*_{re}/*k*_{abs}, where *k*_{re} represents the sum of rearrangement products, e.g., for 2-heptenyl radical, *k*_{re} = *k*_{5,cis} + *k*_{5,trans} + *k*₆. The factor *f* (eq 3) corrects for consumption of hydride from the induced decomposition

(52) Rakowski DuBois, M.; DuBois, D. L.; Vanderveer, M. L.; Haltiwanger, R. C. *J. Inorg. Chem.* **1981**, *20*, 3064.

(53) Ashby, E. C.; DePriest, R. N.; Goel, A. B.; Wenderoth, B.; Pham, T. N. *J. Org. Chem.* **1984**, *49*, 3545–3556.

(54) Coates, R. M.; Johnson, M. W. *J. Org. Chem.* **1980**, *45*, 2685–2697.

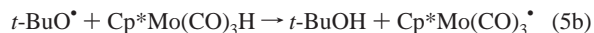
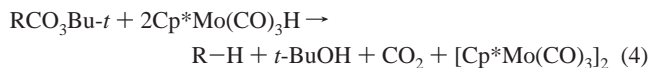
(55) Ashby, E. C.; Bowers, J. R. *J. Am. Chem. Soc.* **1981**, *103*, 2242–2250.

(56) Alnajjar, M. S.; Kuivila, H. G. *J. Am. Chem. Soc.* **1985**, *107*, 416–423.

(57) Rüchardt, C. *Chem. Ber.* **1961**, *94*, 1599.

(58) Rüchardt, C.; Hecht, R. *Chem. Ber.* **1965**, *98*, 2460.

pathway of the peresters forming tert-butyl alcohol. For halide radical precursors, *f* = 1. For peresters, 2 equiv of hydride is consumed for each event of unimolecular perester decomposition (eq 4), or 1 equiv of hydride per chain-reaction-induced decomposition (eqs 5a,b, etc.).



Product concentrations are corrected for temperature-dependent density changes.⁵⁹

Rate Constants for Reaction of Benzyl Radical with Cp*Mo(CO)₃H. Pyrex reaction tubes containing solutions of 0.02 M DBK, 10^{−4} M Cp*Mo(CO)₃H, and 10^{−3} M tert-butylbenzene were freeze–thaw degassed, sealed, and photolyzed with a water-filtered 1-kW high-pressure xenon arc lamp for controlled periods of time (0.50–5.00 ± 0.005 s) using a Uniblitz model 225LOAOT522952 computer-controlled electronic shutter. Reagent concentrations were corrected for solvent vapor pressure and density.^{59,60} Rate constants for hydrogen abstraction were calculated using eq 1c at 0.5–1.5 s photolysis times, using the measured product concentrations, the calculated average molybdenum hydride donor concentration, and the benzyl self-radical termination rate, 2*k*_t, calculated from the expression ln(2*k*_t/M^{−1} s^{−1}) = 27.23 – 2952.5/RT. This expression was calculated using the von Smoluchowski equation modified, eq 6, using the Spornol–Wirtz modification of the Debye–Einstein equation, eq 7, where *f* in eq 7 is the SW microfriction factor.⁶¹

$$2k_t = (8\pi/1000)\sigma\rho D_{AB}N \quad (6)$$

$$D_{AB} = kT/6\pi r_A \eta f \quad (7)$$

Fischer and co-workers^{62–64} have measured self-termination rate expressions for benzyl radical in cyclohexane, ln(2*k*_t/M^{−1} s^{−1}) = 26.2 – 2497.6/RT, and in toluene, ln(2*k*_t/M^{−1} s^{−1}) = 27.05 – 2797.4/RT. For self-termination of benzyl in hexane, we developed the expression ln(2*k*_t/M^{−1} s^{−1}) = 26.0 – 1803.6/RT.⁶⁵ Parameters for estimation of the rate expression employed in these kinetics are presented.⁶⁶ The

(59) Reid, R. C.; Prausnitz, J. M.; Sherwood, T. K. *The Properties of Liquids and Gases*; McGraw-Hill: New York, 1977.

(60) Weast, R. C.; Astle, M. J. *CRC Handbook of Chemistry and Physics*; CRC Press: Boca Raton, FL, 1982–83.

(61) Fischer, H.; Paul, H. *Acc. Chem. Res.* **1987**, *20*, 200–266.

(62) Lehn, M.; Schuh, H.; Fischer, H. *Int. J. Chem. Kinet.* **1979**, *11*, 705–713.

(63) Claridge, R. F. C.; Fischer, H. *J. Phys. Chem.* **1983**, *87*, 1960–1967.

(64) Huggenberger, C.; Fischer, H. *Helv. Chim. Acta* **1981**, *64*, 338–353.

(65) Franz, J. A.; Suleman, N. K.; Alnajjar, M. S. *J. Org. Chem.* **1986**, *51*, 19.

(66) Diffusion coefficients *D*_{AB}, where *D*_{AB} = *kT*/6π*r*_A*ηf*, were calculated for estimation of the self-termination rate of benzyl radical in benzene using the following data. For the radical model, toluene: mp 178 K, bp 383.8 K, MW 92.14, ρ = 6.02 × 10^{−8} cm (average of van der Waals (Edward, J. T. *J. Chem. Educ.* **1970**, *47* (4), 261), LeBas (Ghai, R. L.; Dullien, F. A. L. *J. Phys. Chem.* **1974**, *78*, 2283), and other (Spornol, A.; Wirtz, K. Z. *Naturforsch.* **1953**, *8a*, 522) diameters, σ = 1/4, density of toluene, dens(*T*, K) = 1.1787 – 1.048 × 10^{−3}(*T*, K). For the solvent benzene: mp, 278.7, bp 353.3, MW 78.1, Andrade viscosity, ln(*η*, cP) = −4.117 + 2.0973 × 10³, dens(*T*, K) = 1.192 – 1.059 × 10^{−3}(*T*, K). The microfriction factor *f* of Spornol and Wirtz is given by *f* = (0.16 + 0.4*r*_A/*r*_B)(0.9 + 0.4*T*_A³ – 0.25*T*_B³), and reduced temperatures are given by *T*_X³ = (*T* – *T*_X^f)/(*T*_X^b – *T*_X^f), where *T*_X^f and *T*_X^b are freezing and boiling points of species X = benzyl (A) or benzene (B). The radii in the microfriction factor term are given by *r*_X = (3*V*_X(*χ*)/4π*N*)^{1/3}, where *χ* = 0.74, the volume fraction for cubic closest packed spheres, *V*_X are density-based molecular volumes, and *N* is Avogadro's number. The resulting Smoluchowski expression for self-termination of the benzyl radical in benzene is ln(2*k*_t/M^{−1} s^{−1}) = 27.23 – 2952.47/RT. A similar treatment for benzyl self-termination in toluene is in near-perfect agreement with experimental values (refs 61–64).

absolute error in estimation of self-termination rate constants by this method is estimated to be less than ca. 25%.⁶¹

Acknowledgment. This work supported by the Office of Science, Office of Basic Energy Sciences, Chemical Sciences Division of the U.S. Department of Energy under contract DE-ACO6-76RLO 1830. The authors thank Dr. Donald M. Camaioni for useful discussions and for assembling the computer-

driven optical shutter, and Dr. Tom Autrey for help in preparation of 2,2-dimethylhept-6-enoic acid.

Supporting Information Available: Tabulations of kinetic data for the entries in Table 1 (PDF). This material is available free of charge via the Internet at <http://pubs.acs.org>.

JA991412E